Detecting Localized Plastic Strain by a Scanning Collinear Wave Mixing Method

Guangxin Tang, Minghe Liu, Laurence J. Jacobs & Jianmin Qu

Journal of Nondestructive Evaluation

ISSN 0195-9298

J Nondestruct Eval
DOI 10.1007/s10921-014-0224-1

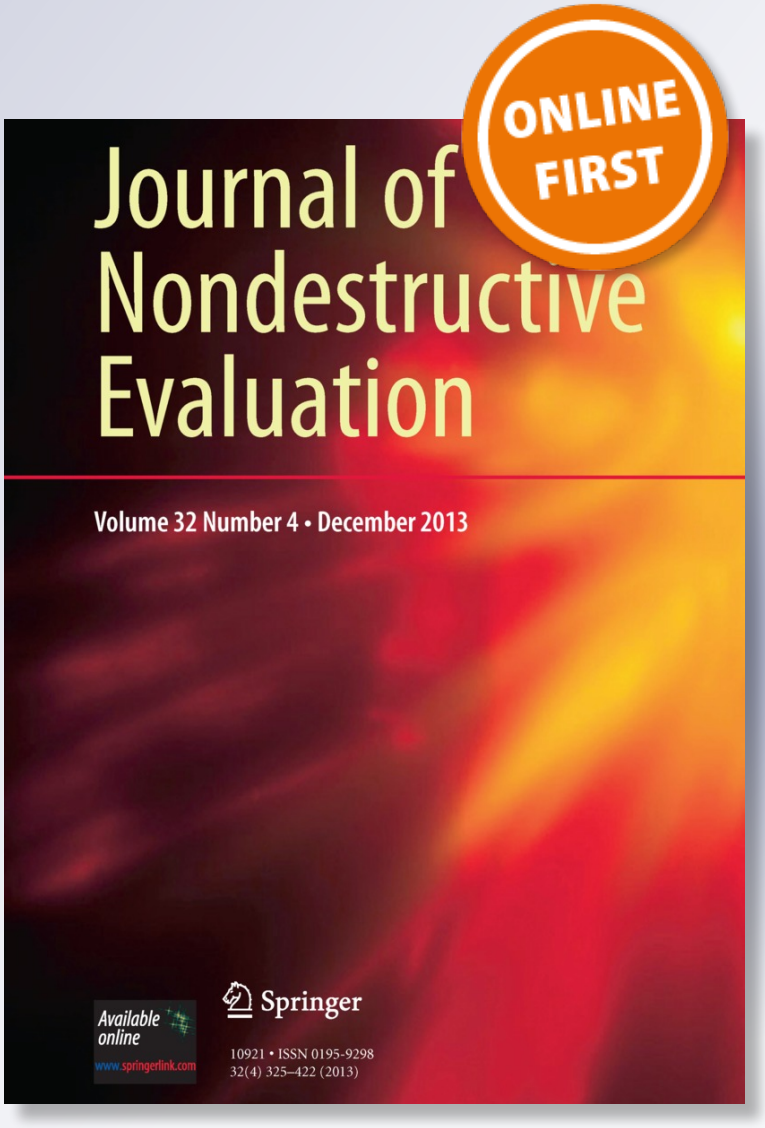

Springer

J Nondestruct Eval
DOI 10.1007/s10921-014-0224-1

Detecting Localized Plastic Strain by a Scanning Collinear Wave Mixing Method

Guangxin Tang · Minghe Liu · Laurence J. Jacobs · Jianmin Qu

Received: 17 November 2013 / Accepted: 6 January 2014

Abstract When the frequencies of a pair of collinear shear and longitudinal waves satisfy the resonant condition, mixing of these two primary waves generates a third, resonant shear wave that propagates in the direction opposite to the propagating direction of the primary shear wave. In this study, experiments were conducted to demonstrate that the acoustic nonlinearity parameter at the location of the mixing zone can be obtained by measuring the resonant shear wave. Since the location of the mixing zone can be controlled by adjusting the trigger time of the transducers that generate the primary waves, this collinear wave mixing technique enables the scanning of a bar sample to measure the distribution of acoustic nonlinearity along the bar. To demonstrate this scanning capability, bar samples with non-uniform acoustic nonlinearity parameters were fabricated by inducing localized plastic deformation at known locations. Scanning collinear wave mixing tests conducted on such bar samples clearly identified the locations of the plastic zone. These results show that collinear wave mixing is a promising method for scanning the test sample to map out the distribution of localized plastic deformation.

Keywords Nonlinear ultrasound · Wave mixing · Plastic deformation · Acoustic nonlinearity parameter

G. Tang · J. Qu (✉)
Department of Mechanical Engineering, Northwestern University, Evanston, IL 60208, USA
e-mail: j-qu@northwestern.edu

M. Liu · J. Qu
Department of Civil and Environmental Engineering, Northwestern University, Evanston, IL 60208, USA

L. J. Jacobs
College of Engineering, Georgia Institute of Technology, Atlanta, GA 30332-0360, USA

1 Introduction

As a longitudinal wave propagates in an elastic solid with quadratic nonlinearity, a second harmonic wave will be generated due to material nonlinearity. The amplitude of the second harmonic wave is proportional to the acoustic nonlinearity parameter of the solid, commonly referred to as β in the literature (1–8). Numerous theoretical studies (8–13) and experimental measurements (8,10,14–20) have demonstrated that β in metallic materials is closely correlated with fatigue damage or cumulative plastic strain in the materials. Such correlation enables the use of nonlinear ultrasound as a tool to characterize fatigue damage in metallic materials nondestructively by measuring the acoustic nonlinearity parameter β.

A widely used technique to measure β is the generation of the second harmonic. In this method, a monochromatic longitudinal wave is sent into the material by a transmitter and the generated second harmonic wave is recorded by a receiver. The measured amplitude of the second harmonic received gives the acoustic nonlinearity parameter. Although this method has been used extensively in the literature, it has two inherent drawbacks. First, this technique can only measure the average β over the region between the transmitter and the receiver. In other words, the method cannot measure the spatial distribution of β. In estimating fatigue life, however, it is often critical to know the localized plastic deformation. Thus, knowing the spatial distribution of β is crucial. Second, the ultrasonic measurement system itself is often nonlinear. Such nonlinearity from the measurement system will generate an additional "instrumentation" second harmonic contribution in the received signal, which cannot be easily separated from the "material" second harmonic generated by the sample being tested. Therefore, great care must be taken to minimize the instrumentation nonlinearity in the measurement system.

Published online: 17 January 2014

To overcome these shortcomings, nonlinear wave mixing techniques were developed (21–24). These techniques are based on the fact that, if the frequencies of two propagating waves satisfy certain resonant or phase-matching conditions, the mixing of these two propagating waves in a nonlinear solid will generate a third propagating wave of a different frequency. This third propagating wave is called the resonant wave. The amplitude of this resonant wave is proportional to the size of the mixing zone and the acoustic nonlinearity parameter of the material in the mixing zone (25). By measuring the amplitude of the resonant wave, the acoustic nonlinearity parameter of the material in the mixing zone can be obtained. Since wave mixing techniques allow certain freedom in selecting the frequency of the resonant wave, it is possible to avoid higher harmonics induced by the nonlinearity of the measurement system. In addition, the measured β is only associated with the acoustic nonlinearity within the mixing zone. This spatial selectivity provides a tool to obtain the spatial distribution of β.

This work presents a scanning collinear wave mixing method where a pair of shear and longitudinal wave transducers are attached to the opposite sides of a sample. Pulses of finite duration are generated by these two transducers. By controlling the trigger time of the transducers, these two opposite-propagating pulses can be controlled to mix at a desired spatial location between these two transducers. When the frequencies of these two propagating pulses satisfy the resonant condition, interactions of these two pulses will generate a third, resonant shear wave that propagates towards the shear wave transducer. The amplitude of this resonant wave is proportional to the acoustic nonlinearity parameter of the material in the mixing zone. By recording the resonant shear wave, the acoustic nonlinearity parameter at the mixing zone is obtained. In what follows, we will first derive the relevant equations for collinear wave mixing in Sect. 2, followed by a description of the fabrication of samples with localized plastic deformation in Sect. 3. The experimental setup for the scanning collinear wave mixing method is presented in Sect. 4, while Sect. 5 gives the measurement results from the scanning collinear wave mixing method. Finally, some concluding remarks are made in Sect. 6.

2 Collinear Wave Mixing

Consider a two-dimensional Cartesian coordinate system xy. For a plane wave propagating in the x-direction, the particle motion is a function of x and t. Thus, the displacement in the x- and y- directions can be written as $u(x,t)$ and $v(x,t)$, respectively. As derived in an early paper (26), the equation of motion can be written as

$$\frac{\partial^2 u}{\partial t^2} - c_L^2 \frac{\partial^2 u}{\partial x^2} = \beta_L c_L^2 \frac{\partial u}{\partial x}\frac{\partial^2 u}{\partial x^2} + \beta_T c_T^2 \frac{\partial v}{\partial x}\frac{\partial^2 v}{\partial x^2}, \tag{1}$$

$$\frac{\partial^2 v}{\partial t^2} - c_T^2 \frac{\partial^2 v}{\partial x^2} = \beta_T c_T^2 \frac{\partial}{\partial x}\left(\frac{\partial u}{\partial x}\frac{\partial v}{\partial x}\right), \tag{2}$$

where $c_L = \sqrt{(\lambda+2\mu)/\rho}$ and $c_T = \sqrt{\mu/\rho}$ are the longitudinal and shear wave velocities, respectively, and

$$\beta_L = 3 + \frac{2(l+2m)}{\lambda+2\mu}, \quad \beta_T = \frac{\lambda+2\mu}{\mu} + \frac{m}{\mu} \tag{3}$$

where λ and μ are the Lamé constants, and l, m, and n are the Murnaghan third order elastic constants. The parameters β_L and β_T are called the acoustic nonlinearity parameters.

Now, consider a time-harmonic longitudinal wave u_1 propagating in the negative x-direction and a time-harmonic shear wave v_1 propagating the positive x-direction,

$$u_1 = U\sin\left[\omega_L\left(t+\frac{x}{c_L}\right)\right], \quad v_1 = V\sin\left[\omega_T\left(t-\frac{x}{c_T}\right)\right] \tag{4}$$

where U and V are given constants, and ω_T and ω_L are the circular frequencies for the shear and longitudinal waves, respectively. Substituting (4) into (2) and neglecting higher order terms, we arrive at the governing equation for the mixing wave

$$\begin{aligned}\frac{\partial^2 v_2}{\partial t^2} - c_T^2 \frac{\partial^2 v_2}{\partial x^2} &= \beta_T c_T^2 \frac{\partial}{\partial x}\left(\frac{\partial u_1}{\partial x}\frac{\partial v_1}{\partial x}\right) \\ &= \frac{\beta_T U V \omega_L \omega_T c_T}{2c_L}[k_+\sin(\omega_- t + k_+ x) \\ &\quad + k_-\sin(\omega_+ t + k_- x)],\end{aligned} \tag{5}$$

$$\begin{aligned}\frac{\partial^2 v_2}{\partial t^2} - c_T^2 \frac{\partial^2 v_2}{\partial x^2} &= \beta_T c_T^2 \frac{\partial}{\partial x}\left(\frac{\partial u_1}{\partial x}\frac{\partial v_1}{\partial x}\right) \\ &= B_1\sin(\omega_- t + k_+ x) \\ &\quad + B_2\sin(\omega_+ t + k_- x)\end{aligned} \tag{6}$$

where $\omega_\pm = \omega_L \pm \omega_T$ and $k_\pm = \omega_L/c_L \pm \omega_T/c_T$. One of the particular solutions to (6) is

$$v_2 = \frac{\beta_T U V \omega_L \omega_T c_T k_+}{2c_L(c_T k_+ - \omega_-)(c_T k_+ + \omega_-)}\sin(\omega_- t + k_+ x). \tag{7}$$

If the forcing frequency $\omega_- \to k_+ c_T$, then the amplitude of v_2 approaches infinity. This is similar to the resonant vibration of an elastic string if $k_+ c_T$ were viewed as the "natural frequency" of the system. It is straightforward to show (26) that the resonant condition $\omega_- = c_T k_+$ leads to

$$\frac{\omega_L}{\omega_T} = \frac{2c_L}{c_L - c_T}. \tag{8}$$

Physically, satisfaction of (8) ensures that the phase velocity ω_-/k_+ of the forcing term matches the shear wave phase velocity c_T, i.e., $\omega_-/k_+ = c_T$, so that the generated mixing wave accumulates as it propagates. Therefore, Eq. (8) is

also called the phase-matching condition. Similar phenomena also occur in nonlinear Lamb waves, e.g., (18).

If the frequencies of the two primary waves satisfies the resonant or phase-matching condition (8), mixing of these two waves will generate a third, higher order shear wave v_2 propagating in the negative x-direction,

$$v_2 = A\cos\left[\omega_R\left(t + \frac{x}{c_T}\right)\right], \tag{9}$$

where

$$A = \frac{\beta_T U V \omega_T^2 x}{2c_T(c_L - c_T)},\ \omega_R = \frac{c_L + c_T}{c_L - c_T}\omega_T = \omega_L - \omega_T. \tag{10}$$

Here we have neglected the higher order terms that do not grow with increasing propagation distance. Notice that the phase velocity of v_2 is the shear wave velocity, c_T.

The above derivation assumes that the two primary waves are plane waves of infinite duration. In practice, the two primary waves are pulses with finite duration. In this case, the zone where the two primary waves mix is finite. Thus, the x in the expression of A in (10) should be replaced by a characteristic length l_m that is related to the size of the mixing zone, i.e.,

$$A = \frac{\beta_T U V \omega_T^2 l_m}{2c_T(c_L - c_T)}. \tag{11}$$

Once the resonant wave v_2 is generated within the mixing zone, it will propagate as a propagating shear wave of frequency ω_R in the negative x-direction. Since v_2 is generated at the mixing zone, its amplitude A carries the information about the acoustic nonlinearity parameter β_T at the mixing zone. By measuring A, the acoustic nonlinearity parameter β_T of the material in the mixing zone can be obtained through

$$\beta_T = \frac{2c_T(c_L - c_T)}{U V \omega_T^2 l_m} A. \tag{12}$$

By controlling the location of the wave mixing zone, the acoustic nonlinearity parameter β_T at a desired spatial location within a sample can be obtained. This is the theoretical basis for the scanning collinear wave mixing technique.

3 Sample Preparation

The samples used in this study are circular cross-section bars made of Al-6061. Sample 0 has a diameter of 25.4 mm. Its acoustic nonlinearity parameter is uniform throughout the sample. Samples 1, 2 and 3 all have the same diameter, 25.4 mm. But their acoustic nonlinearity parameter is not uniform along the axial direction of the bar. These samples with non-uniform acoustic nonlinearity parameters will be used to demonstrate the scanning capability of the proposed collinear wave mixing method.

To fabricate a sample with a non-uniform acoustic nonlinearity parameter, we considered the earlier studies, e.g., (8,10,14–20), that show a correlation between plastic deformation and the acoustic nonlinearity parameter. Thus, samples with localized plastic deformation will have a non-uniform acoustic nonlinearity parameter. Therefore, to make samples with non-uniform acoustic nonlinearity parameter, we fabricated samples with localized plastic deformation.

Specifically, three bar samples of Al-6061 with diameter D and length $L = L_1 + L_2$ were obtained, see Fig. 1. A notch was machined on each sample. The depth and width of the notch are $(D-d)/2$ and g, respectively, and the center of the notch is L_1 distance away from the left end, see Fig. 1. Three such samples were made. Their geometrical dimensions are listed in Table 1.

These notched samples were then subjected to uniaxial tensile load above the yield strength to create plastic deformation near the notch. After the uniaxial tension was applied (and removed), the notched samples were carefully machined to remove the notch by machining off the "outer shell," see Fig. 1. The final sample is thus a smooth circular cross-section bar of diameter d that contains a plastic zone at a known location.

When the notched bar is subjected to uniaxial loading, the strain is not uniform along the bar because of the notch. To determine the load magnitude needed for plastic deformation near the notch, and to understand the extent of the plastic zone, uniaxial tensile tests were conducted on a circular cross-section bar made from the same Al-6061. A typical

Table 1 Sample geometries

Samples	D (mm)	d (mm)	g (mm)	L_1 (mm)	L_2 (mm)	Plastic strain (%)
1	38.1	25.4	20	85	104	3
2	38.1	25.4	20	94	89	5
3	38.1	25.4	46	86	94	6

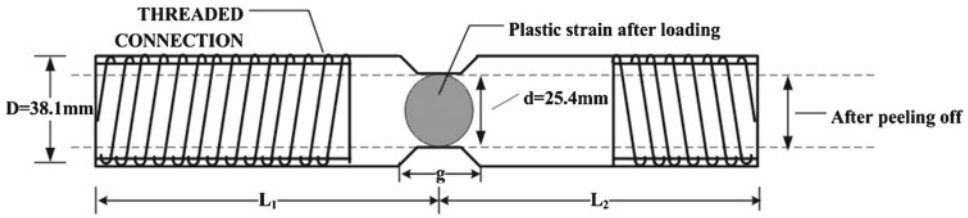

Fig. 1 Sample for tensile loading

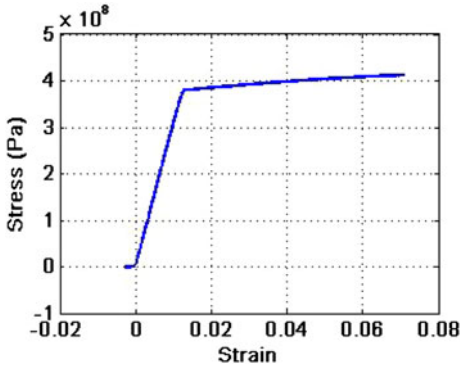

Fig. 2 Stress–strain curve of Al-6061

stress–strain curve obtained from the tensile tests is shown in Fig. 2.

Based on the stress–strain curve shown in Fig. 2, the finite element method was used to calculate the elastic-plastic deformation of the notched sample. The commercial software ANSYS was used for this purpose. Contour plots of the plastic (Von Mises) strain are shown in Fig. 3. It is seen that plastic deformation is highly localized to the neck region of the notch. To better quantify the plastic deformation, we plotted in Fig. 4 the plastic strain distribution along the center line of the bar sample. In this plot, the location $x = 1$ corresponds to the center of the notch in each sample. It is seen that the maximum plastic strains are 3, 5 and 6 % for the three samples, respectively. These values are well beyond the yield strain of the material as shown in Fig. 2.

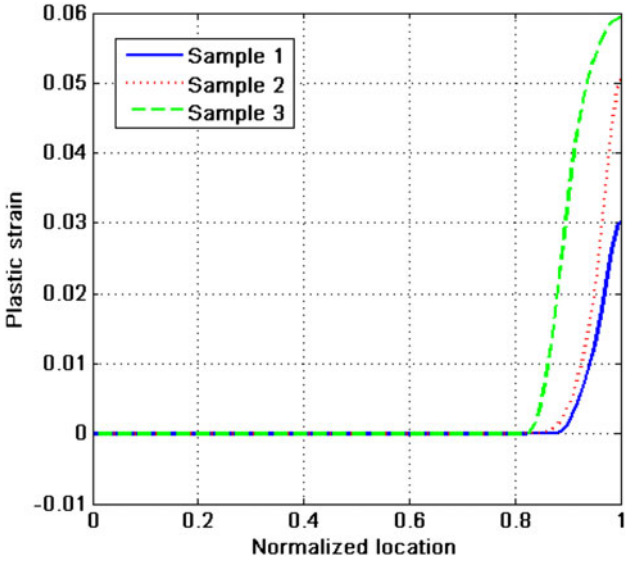

Fig. 4 Plastic strain distribution along the axis of the notched sample

4 Experimental Setup

The experimental setup developed in (26) is schematically shown in Fig. 5. The RAM-5000 SNAP (RITEC Inc., Warwick, RI) is used as the signal generator. The internal trigger of the SNAP system is used as the reference trigger. A broad band shear wave transducer (diameter = 12.7 mm) with a center frequency of 5 MHz is connected to channel 1 of the signal generator through a RDX-6 diplexer (RITEC Inc., Warwick, RI), which enables the shear wave transducer to serve as both a transmitter and a receiver. A longitudinal transducer (diameter = 12.7 mm) with center frequency of 10 MHz is connected to channel 2 of the signal generator. The resonant wave received by the shear wave transducer is sent to the oscilloscope and the digitized signal is then sent to the computer for signal processing.

The test samples described in the previous section were used in the mixing tests. A shear wave transducer is attached to one end of the bar sample, sending a 5-cycle tone burst (6.3 mm spatially) with frequency $f_T = \omega_T/2\pi = 2.5$ MHz. The longitudinal wave transducer is attached to the other end of the sample, sending a 9-cycle tone burst (5.9 mm spatially) with frequency $f_L = \omega_L/2\pi = 9.65$ MHz. These

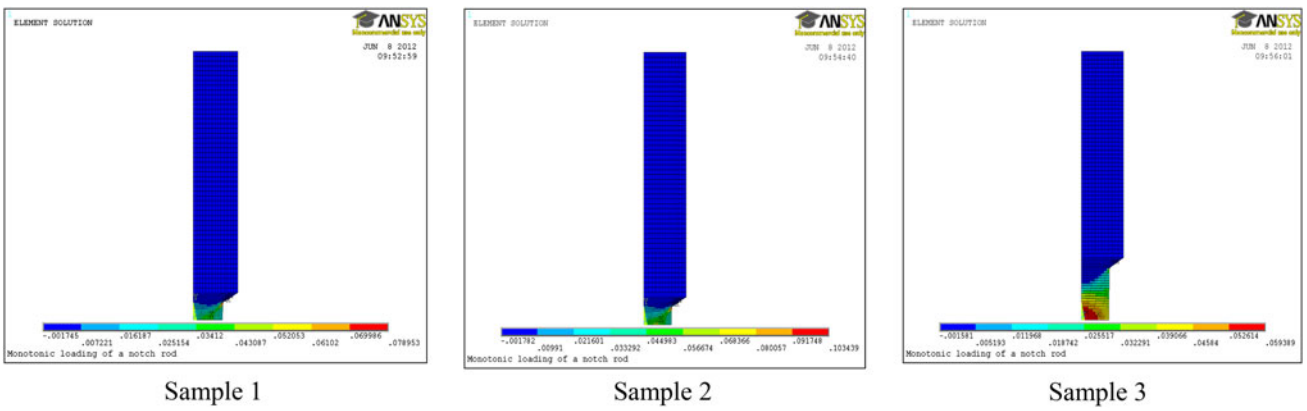

Fig. 3 Contour plots of plastic strain for the notched samples

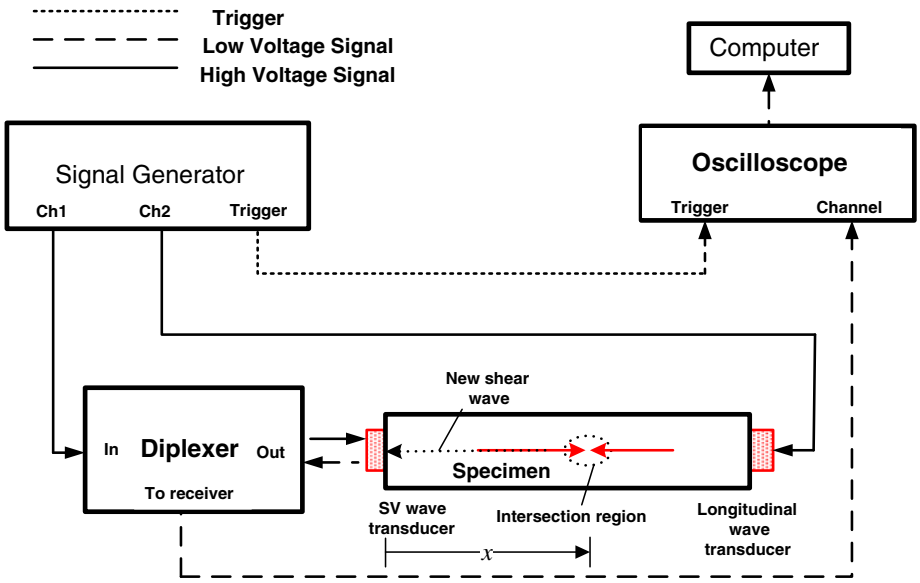

Fig. 5 Schematic of experimental setup for the collinear wave mixing method

two frequencies satisfy the resonant condition given by (8) for the sample material. Therefore, when these two primary waves mix at a desired spatial location, their mixing generates a third, resonant shear wave that propagates towards the shear wave transducer. As discussed in the previous section, the amplitude of this resonant shear wave is proportional to the acoustic nonlinearity parameter β_T at the location where the two primary waves mix. Moving the mixing zone from one end of the sample to the other generates a scan of β_T along the bar sample. To improve the signal to noise ratio, the pulse-inversion technique (15) is used to enhance the even order wave v_2 by adding two sets of 180° out-of-phase signals.

A typical time-domain resonant wave signal received by the shear wave transducer using the aforementioned procedure is shown in Fig. 6a and its frequency spectrum is shown in Fig. 6b. The solid red line in Fig. 6a shows the resonant wave received by the shear wave transducer, while the dashed blue line is the signal after applying a Hanning window to the original time-domain signal to help smooth the frequency-domain signal shown in Fig. 6b. From Fig. 6b, we can see that the center frequency of the resonant wave packet is 7.15 MHz, which is equal to $f_R = \omega_R/2\pi = f_L - f_T$, the difference frequency of the two primary waves. The amplitude at 7.15 MHz in Fig. 6b is proportional to the amplitude A of the resonant shear wave generated by the mixing of the two primary waves, see (9)–(10). Thus, knowing the amplitude at 7.15 MHz in Fig. 6b enables us to calculate the acoustic nonlinearity parameter β_T from (12). This β_T is associated with the material in the mixing zone. Further, by adjusting the trigger time of the two transducers, the two primary waves can mix at different locations throughout the sample. Thus β_T can be obtained as a function of location x.

5 Results and Discussions

First, to illustrate the collinear wave mixing method described in the previous section, measurements were carried out on Sample 0. Note that Sample 0 is homogeneous in that its acoustic nonlinearity parameter is uniform throughout the sample. By adjusting the delay time of the two transducers, we moved the location of the mixing zone from the left (near the shear wave transducer) to the right incrementally. This allows the measurement of the amplitude of the resonant shear wave as a function of position x, i.e., $A(x)$. Showing in Fig. 7 is the normalized amplitude $\bar{A}(x) = A(x)/A(x_0)$, where x_0 is the location of the first measurement point. In this particular case, $x_0 = 37.9$ mm.

We note that, according to the theoretical derivations given by (1)–(11), the amplitude A should be independent of the location of the mixing zone if the sample is uniform, i.e., the acoustic nonlinearity parameter is a constant throughout the sample. However, the theoretical derivation is based on the assumption that the wave packets are plane waves, and that the material is linear elastic without energy loss. In the actual test, the waves generated by the transducers are beams of finite diameter, and the material has loss. Wave beams of finite diameter tend to diverge as they propagate and material loss causes signal attenuation. In addition, the bar sample also acts as a waveguide, so the propagating wave is no longer planar. In other words, the amplitudes of the primary waves U and V are both functions of locations. It thus follows from (11) that A will depend on the location of the mixing zone even though the acoustic nonlinearity parameter β_T is a constant throughout the sample.

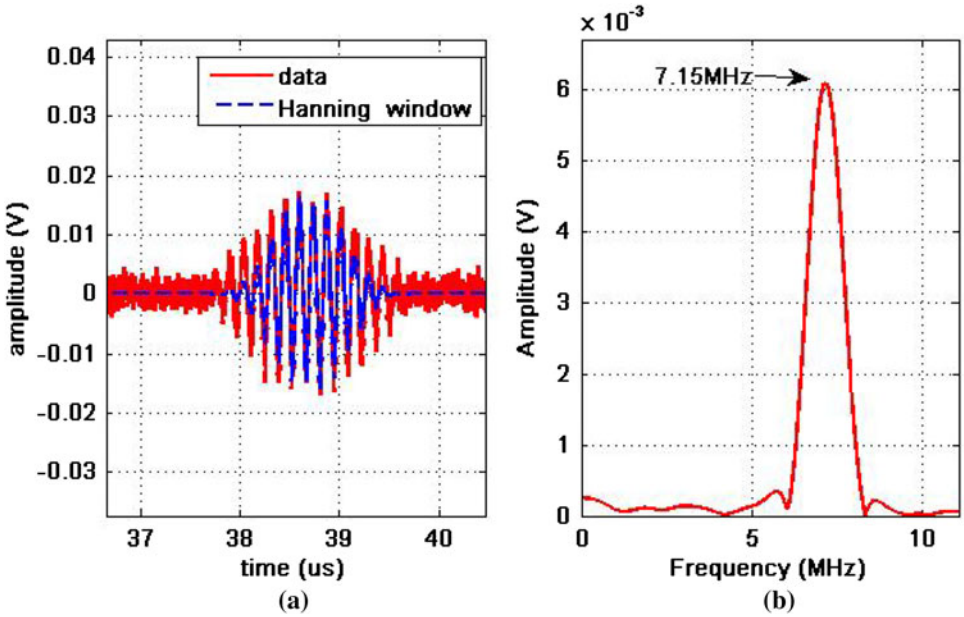

Fig. 6 **a** Resonant wave received by the shear wave transducer (*red solid line*) and the same signal after applying a Hanning window (*blue dashed line*), **b** frequency spectrum of the resonant wave after applying a Hanning window (Color figure online)

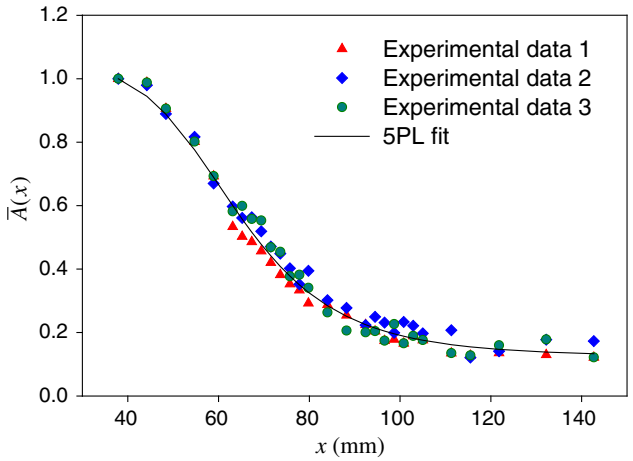

Fig. 7 Normalized amplitude of the resonant shear wave as a function of location x in a uniform bar sample

Several curve fitting techniques were investigated to fit the experimental data shown in Fig. 7. It turns out that the five-parameter logistic (5PL) function (27) seems to provide a good fit to the experimental data shown in Fig. 7. Although it is unclear why this is the case, the 5PL function will be used as a baseline for A. Any deviation of A from the 5PL function would indicate a non-uniform spatial distribution of β_T. Symbolically, one may re-write (11) as

$$A(x) = \beta_T(x) f(x), \tag{13}$$

where x indicates the location of mixing zone and $f(x)$ is a 5PL function. It then follows that the normalized acoustic nonlinearity parameter is given by

$$\bar{\beta}_T(x) = \frac{\beta_T(x)}{\beta_T(x_0)} = \frac{\bar{A}(x)}{\bar{f}(x)}, \tag{14}$$

where $\bar{A}(x) = A(x)/A(x_0)$ and $\bar{f}(x) = f(x)/f(x_0)$ with x_0 being the location of the first measurement point. It is now clear from (14) that if $\bar{A}(x) \propto \bar{f}(x)$ is a 5PL function as shown in Fig. 7, then β_T will be independent of x. Vice versa, if $\bar{A}(x)$ deviates from a 5PL function, $\bar{\beta}_T(x)$ will depend on x.

We note that the experimental data showing in Fig. 7 are from three tests. After each test, the transducers are completed detached and the sample was cleaned to remove any residual couplant before the next test.

Next, we carried out similar tests on Samples 1, 2 and 3. The amplitude A from these samples is plotted as a function of x in Fig. 8. Figure 8a is from Sample 1. Fig. 8b is also from Sample 1, but the positions of the shear wave and longitudinal wave transducers are switched so that the distance between the shear wave transducer (receiver) and the location of the plastic zone is different between Fig. 8a, b. In obtaining Fig. 8a, the center of the plastic zone is 85 mm from the shear wave transducer and 104 mm away from the longitudinal wave transducer. In obtaining Fig. 8b, the center of plastic zone is 104 mm from the shear wave transducer and 85 mm away from the longitudinal wave transducer. Figure 8c, d are from Samples 2 and 3, respectively.

In all these figures, the dots are experimental data points, and the solid lines are the best fit using the 5PL function. In obtaining the best 5PL fit, data within the notched region were excluded. All experimental data are an average of three sets of tests. The location of the plastic zone center is indicted by the vertical dash-lines in these figures. It is seen from Fig. 8 that for the samples that have a localized plastic zone, the amplitude of the resonant shear wave no longer behaves like a 5PL function of x. The region over which $\bar{A}(x)$ deviates from the

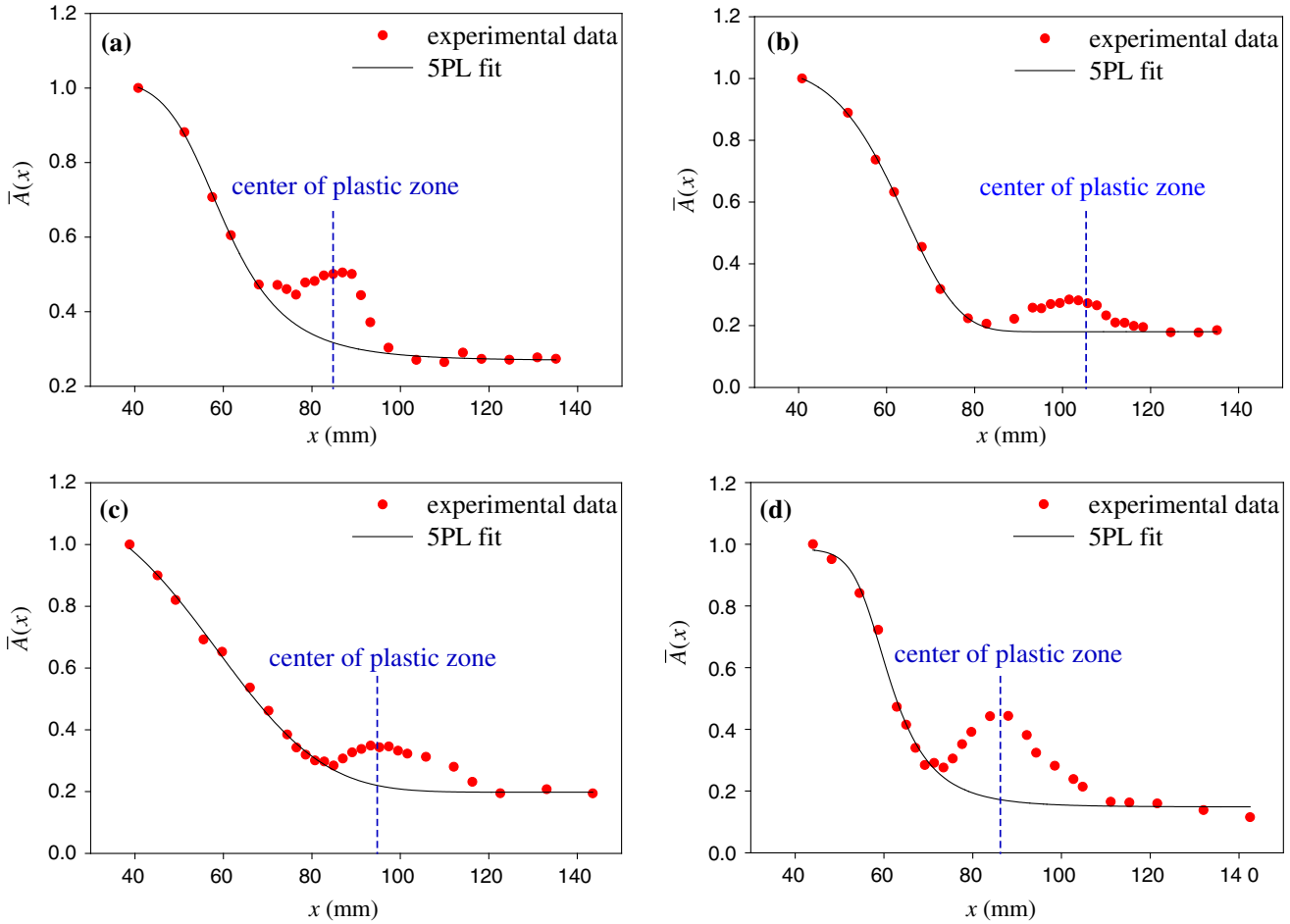

Fig. 8 Normalized amplitude of the resonant shear wave $\bar{A}(x)$; **a** from Sample 1 (center of plastic zone is at x = 85 mm), **b** from Sample 1 (center of plastic zone is at x = 104 mm), **c** from Sample 2 (center of plastic zone is at x = 94 mm), and **d** from Sample 3 (center of plastic zone is at x = 86 mm)

5PL function coincides exactly with the location of the plastic zone, indicating that the acoustic nonlinearity β_T in the plastic zone differs from its values elsewhere in the sample.

To close this section, we note that the magnitudes of the plastic strains in Samples 1, 2 and 3 are different, ranging from 3 to 6 %. Unfortunately, such differences were not captured by the experimentally measured magnitudes of the amplitudes of resonant shear wave in our results, as they should be according to the theory. Measurement errors certainly contributed to this inaccuracy. But, we believe the main reason is the lack of accurate knowledge of the baseline. In the proceeding discussions, we used the 5PL function fit as the baseline, which may not be quantitative enough to discern the differences induced by the different plastic strain levels.

6 Summary and Concluding Remarks

In this study, experiments were conducted to demonstrate that the acoustic nonlinearity parameter at the location of the mixing zone can be obtained by measuring the resonant wave generated by two collinearly propagating primary shear and longitudinal pulses. Since the location of the mixing zone can be controlled by adjusting the trigger time of the transducers that generate the primary waves, this collinear wave mixing method enables the scanning of a bar sample to measure the distribution of acoustic nonlinearity along the bar. To demonstrate this scanning capability, bar samples with non-uniform acoustic nonlinearity parameter were fabricated by inducing localized plastic deformation at known locations. Scanning collinear wave mixing tests conducted on such bar samples clearly identified the locations of the plastic zone nondestructively. These results show that collinear wave mixing is a promising method for scanning a test sample to map out the distribution of localized plastic deformation.

It should be noted that the results reported here represent only a preliminary investigation. More work is needed to optimize the measurement method. Several key steps of further studies are discussed below.

First, we note from (11) that the amplitude of the resonant wave is proportional to the size of the wave mixing zone l_m. In other words, a large mixing zone would increase the signal-to-noise-ratio. However, for scanning purposes, a smaller mixing zone would increase the spatial resolution of the scan. Thus, a compromise will need to be made between measurement accuracy and spatial resolution. In the work presented here, the shear wave pulse is a 5-cycle tone burst (6.3 mm spatially) with a frequency of $f_T = 2.5$ MHz, and the longitudinal wave pulse is a 9-cycles tone burst (5.9 mm) with a frequency of $f_L = 9.65$ MHz. Based on the phase velocities of these two primary waves in Al-6061, the maximum mixing zone is calculated to be $l_m = 6.1$ mm. This particular set of parameters was chosen so that the size of the mixing zone is roughly the same as the size of the plastic zone in the sample. In practice, the size of the plastic zone is often an unknown quantity to be identified by the scanning collinear wave mixing method. Thus a method is needed to estimate the size of the mixing zone a priori.

Second, the collinear mixing method reported here uses two opposite-propagating primary waves. This requires that the transducers be mounted on the opposite ends of the bar sample, which means that access to both side of the sample is needed. This prevents the application of the proposed method to situations where access to only one side of the sample is available. More importantly, such an opposite-propagating configuration requires careful alignment of the two transducers. This has proven to be extremely difficult. To overcome these two drawbacks, one may consider placing both transducers on the same side of the sample. It can be shown analytically that the resonant shear wave still propagates back to the shear wave transducer even when both transducers are mounted on the same side of the sample. Clearly, the challenge here is to have a transducer that can generate both longitudinal and shear wave from the same spot on the sample. We have fabricated two such transducers. In one, the longitudinal and shear wave piezoelectric elements are placed side by side, and in the other they are placed concentrically. Measurement results from these dual element transducers will be reported elsewhere.

Finally, as discussed earlier, the wave beams generated by the transducers tend to diverge as the waves propagate, which makes the amplitude of the primary waves vary with propagation distance. This creates difficulties in interpreting the scanning results. To overcome these difficulties, numerical simulations to quantify this linear beam divergence are needed so we can know how the amplitude of the resonant wave varies when the material is homogeneous. This will provide an accurate baseline for interpreting the results when the material is not homogeneous. Without such a baseline, it is difficult to estimate the magnitude of the deviation that is caused by the non-uniform distribution of the acoustic nonlinearity parameter as opposed to the beam divergence.

Acknowledgments The research was supported in part by the US DoE Nuclear Energy University Program through contracts 00127346 and 00126931.

References

Lamb, H.: Dynamical Theory of Sound, pp. 177–185. Edward Arnold and Company, London (1925)

Keck, W., Beyer, R.T.: Frequency spectrum of finite amplitude ultrasonic waves in liquids. Phys. Fluids **3**(3), 346–352 (1960)

Breazeale, M.A., Thompson, D.O.: Finite-Amplitude Ultrasonic Waves in Aluminum. Appl. Phys. Lett. **3**(5), 77–78 (1963)

Thurston, R.N., Shapiro, M.J.: Interpretation of ultrasonic experiments on finite-amplitude waves. J. Acoust. Soc. Am. **41**(4p2), 1112–1125 (1967)

Thompson, R.B., Buck, O., Thompson, D.O.: Higher harmonics of finite-amplitude ultrasonic-waves in solids. J. Acoust. Soc. Am. **59**(5), 1087–1094 (1976)

Thompson, R.B., Tiersten, H.F.: Harmonic-generation of longitudinal elastic-waves. J. Acoust. Soc. Am. **62**(1), 33–37 (1977)

Cantrell Jr, J.H.: Acoustic-radiation stress in solids. I. Theory. Phys. Rev. B **30**(6), 3214–3220 (1984)

Cantrell, J.H.: Fundamentals and applications of nonlinear ultrasonic nondestructive evaluation. In: Kundu, T. (ed.) Ultrasonic Nde for Engineering and Biological Material Characterization, pp. 311–362. CRC, Boca Raton (2004)

Hikata, A., Chick, B.B., Elbaum, C.: Dislocation contribution to the second harmonic generation of ultrasonic waves. J. Appl. Phys. **36**, 229–236 (1965)

Kim, J.Y., Qu, J., Jacobs, L.J., Littles, J.W., Savage, M.F.: Acoustic nonlinearity parameter due to microplasticity. J. Nondestruct. Eval. **25**, 28–36 (2006)

Hikata, A., Elbaum, C.: Generation of ultrasonic second and third harmonics due to dislocations I. Phys. Rev. **144**, 469–477 (1966)

Hikata, A., Sewell, F.A., Elbdum, C.: Generation of ultrasonic second and third harmonics due to dislocations Ii. Phys. Rev. **151**, 442–449 (1966)

Suzuki, T., Hikata, A., Elbaum, C.: Anharmonicity due to glide motion of dislocations. J. Appl. Phys. **35**, 2761–2766 (1964)

Herrmann, J., Kim, J.Y., Jacobs, L.J., Qu, J., Littles, J.W., Savage, M.: Assessment of material damage in a nickel-base superalloy using nonlinear Rayleigh surface waves. J. Appl. Phys. **99**, 124913 (2006)

Kim, J.Y., Jacobs, L.J., Qu, J., Littles, J.W.: Experimental characterization of fatigue damage in a nickel-base superalloy using nonlinear ultrasonic waves. J. Acoust. Soc. Am. **120**, 1266–1273 (2006)

Bermes, C., Kim, J.Y., Qu, J., Jacobs, L.J.: Experimental characterization of material nonlinearity using lamb waves. Appl. Phys. Lett. **90**(2), 021901 (2007)

Pruell, C., Kim, J.Y., Qu, J., Jacobs, L.J.: Evaluation of plasticity driven material damage using lamb waves. Appl. Phys. Lett. **91**(23), 231911 (2007)

Bermes, C., Kim, J.Y., Qu, J., Jacobs, L.J.: Nonlinear lamb waves for the detection of material nonlinearity. Mech. Syst. Signal Process. **22**(3), 638–646 (2008)

Liu, M., Kim, J.Y., Jacobs, L.J., Qu, J.: Experimental study of nonlinear Rayleigh wave propagation in shot-peened aluminum plates-feasibility of measuring residual stress. Ndt E Int. **44**(1), 67–74 (2011)

Littles Jr, J.W., Jacobs, L.J., Qu, J.: Experimental and theoretical investigation of scattering from a distribution of cracks. Ultrasonics **33**(1), 37–43 (1995)

Rollins, F.R.: Interaction of ultrasonic waves in solid media. Appl. Phys. Lett. **2**(8), 147–148 (1963)

Rollins, F.R., Todd, P.H., Taylor, L.H.: Ultrasonic study of 3-phonon interactions. 2. Experimental results. Phys. Rev. **136**(3A), A597–A601 (1964)

Taylor, L.H., Rollins, F.R.: Ultrasonic study of 3-phonon interactions. I. Theory. Phys. Rev. **136**(3A), A591–A596 (1964)

Croxford, A.J., Wilcox, P.D., Drinkwater, B.W., Nagy, P.B.: The use of non-collinear mixing for nonlinear ultrasonic detection of plasticity and fatigue. J. Acoust. Soc. Am. **126**(5), El117–El122 (2009)

Jones, G.L., Korbett, D.R.: Interaction of elastic waves in an isotropic solid. J. Acoust. Soc. Am. **35**(1), 5–10 (1963)

Liu, M., Tang, G., Jacobs, L.J., Qu, J.: Measuring acoustic nonlinearity parameter using collinear wave mixing. J. Appl. Phys. **112**, 024908 (2012)

Dudley, R.A., Edwards, P., Ekins, R.P., Finney, D.J., McKenzie, I.G.M., Raab, G.M., Rodbard, D., Rodgers, R.P.C.: Guidelines for immunoassay data processing. Clin. Chem. **31**, 1264–1271 (1985)